Marine Pollution Bulletin 70 (2013) 140–146

Contents lists available at SciVerse ScienceDirect

Marine Pollution Bulletin

journal homepage: www.elsevier.com/locate/marpolbul

Estimating sub-surface dispersed oil concentration using acoustic backscatter response

Christopher B. Fuller [a,*], James S. Bonner [a], Mohammad S. Islam [a], Cheryl Page [b], Temitope Ojo [a], William Kirkey [a]

[a] Civil and Environmental Engineering, Clarkson University, 8 Clarkson Ave., Potsdam, NY 13699, USA
[b] Texas A&M University, College Station, TX 77843-3136, USA

ARTICLE INFO

Keywords:
Dispersed oil
Droplet size distribution
Acoustic backscatter
ADCP
LISST-100

ABSTRACT

The recent *Deepwater Horizon* disaster resulted in a dispersed oil plume at an approximate depth of 1000 m. Several methods were used to characterize this plume with respect to concentration and spatial extent including surface supported sampling and autonomous underwater vehicles with *in situ* instrument payloads. Additionally, echo sounders were used to track the plume location, demonstrating the potential for remote detection using acoustic backscatter (ABS). This study evaluated use of an Acoustic Doppler Current Profiler (ADCP) to quantitatively detect oil-droplet suspensions from the ABS response in a controlled laboratory setting. Results from this study showed log-linear ABS responses to oil-droplet volume concentration. However, the inability to reproduce ABS response factors suggests the difficulty in developing meaningful calibration factors for quantitative field analysis. Evaluation of theoretical ABS intensity derived from the particle size distribution provided insight regarding method sensitivity in the presence of interfering ambient particles.

1. Introduction

In April 2010, the *Deepwater Horizon* blowout resulted in the largest off-shore oil spill in history, releasing nearly 5 million barrels of oil into the Gulf of Mexico (Lubchenco, 2010). The blowout occurred at the well head at a depth of 1500 m, where the oil dispersant Corexit® 9500 was injected (Hazen et al., 2010). This subsurface spill produced a suspended oil plume between 1030 and 1300 m depth that was identified using autonomous underwater vehicles (AUVs) and cable-lowered sampling rosettes (Camilli et al., 2010). Sonar surveys showed acoustic signatures attributed to oil plumes near the well head (Smith et al., 2010) demonstrating the capacity to use acoustic backscatter to detect sub-merged oil plumes. Acoustic backscatter (ABS) obtained using Acoustic Doppler Current Profilers (ADCPs) has previously been evaluated as a surrogate method to quantify suspended solids concentration (Wall et al., 2006; Gartner, 2004; Gray and Gartner, 2009; Hamilton et al., 1998). It has also been demonstrated that oil dispersed in the water occurs predominantly as a droplet suspension (Page et al., 2000; Sterling et al., 2004a,b,c, 2005). Thus, suggesting that ABS techniques may also be employed to quantify dispersed oil plumes.

ABS signal strength is a function of the particle size distribution and concentration and can be calculated using the expression for Rayleigh target strength

$$TS_R = 10 Log I_0 \left(\frac{\pi^2}{\lambda^4} \left(1 + \frac{3}{2}\mu \right)^2 \sum_{p=1}^{n} \left(\frac{4}{3} \left(\frac{d_p}{2} \right)^3 \pi \right)^2 \right) \quad (1)$$

where I_0 is the ADCP echo intensity at the source minus the transmission losses due to beam spreading and water absorption, λ the acoustic wave length, μ the cosine of the angle between the scattering directions and the reverse direction of the incident wave, n the number of particles, and d_p is the diameter of individual particle (Urick, 1983; Reichel and Nachtnebel, 1994). This expression assumes small spherical particles where the circumference is much less than the acoustic wavelength. Sterling et al. (2004a) previously showed that dispersed oil suspensions generated at mean shear rates typical of marine and estuarine systems were composed of spherical droplets with circumferences on the order of 75 μm, thus satisfying the conditions required for Rayleigh scattering with 2400 kHz signal. While the primary condition suggesting that ABS can be used to measure sub-surface dispersed oil plumes is satisfied, there are two principles that can negatively affect this application.

* Corresponding author. Tel.: +1 315 261 2172.
E-mail address: cfuller@clarkson.edu (C.B. Fuller).

0025-326X/$ - see front matter © 2013 Elsevier Ltd. All rights reserved.
http://dx.doi.org/10.1016/j.marpolbul.2013.02.025

First, sound absorption causes acoustic backscatter intensity to decay exponentially with range and the level of absorption increases proportionally to the frequency (Urick, 1983). Thus, lower frequency signals are required for more distant (i.e. deeper) ABS measurements. For example, the nominal range of the 2400 kHz StreamPro is 2 m (RD Instruments, 2006) while the nominal range of the 76.8 kHz ADCP is 700 m (RD Instruments, 1996). This limitation restricts surface detection of deep sub-surface oil plumes to acoustic instruments with frequencies on the order of 38 kHz with a range of 800–1000 m (Teledyne RD Instruments, 2010).

The second principle affecting remote dispersed oil plume detection with ABS technology is a function of the Rayleigh target strength equation which indicates that the ABS intensity is proportional to the fourth power of the droplet radius and inversely proportional to the sixth power of the acoustic wavelength (Urick, 1983). Therefore, the ABS intensity from a droplet of a given size would be significantly less when measured with a longer wavelength (lower frequency) instrument compared to shorter wavelength instrument. For example, the theoretical Raleigh target strength from a single 100 μm diameter droplet at 2400 kHz and 38 kHz would be 0.63 decibels (dB) and −71 dB, respectively. Another benefit provided by decreasing the acoustic frequency is an increase in the maximum droplet diameters responsible for Rayleigh scattering, defined as when the ratio of droplet circumference to wavelength is unity (Urick, 1983). Applying this convention dictates that maximum droplet diameters for 2400 kH and 38 kH signals are approximately 200 and 12,000 μm, respectively. The lower frequency ADCPs are capable of detecting sub-surface oil plumes consisting of large droplets, but would be limited in detecting plumes consisting of small droplets. These conflicting processes must be balanced to effectively apply ABS as a viable remote oil sensing methodology.

Camilli et al. (2010) found that the sub-surface oil plume resulting from the Deepwater Horizon spill persisted for months indicating that the plume was residing in a stable water column stratum. The strength of this stratification, is a function of the density and shear gradients and may be described using the Richardson number (*Ri*) (Islam et al., 2010). When the density gradient is much stronger than shear gradient, the stratification will be well defined and the diffusion of the small oil droplets into the surrounding strata will be limited. The presence of shear-structure within the water column has been shown to result in elevated diffusivity values compared to relative diffusivity values determined for turbulence alone (Ojo et al., 2006). Therefore, plume persistence over extended periods indicates that shear within the plume was minimal. Considering that droplet collision efficiency (i.e. aggregation) is dominated by shear (Sterling et al., 2004a) implies that droplet aggregation would be minimized thereby reinforcing the presence of a stable oil droplet suspension. In shear dominated systems droplet aggregation would be enhanced, leading to the formation of larger droplets with subsequent increases in both vertical settling velocities and diffusion (Sterling et al., 2004a; Ojo et al., 2006). From the perspective of using ABS intensity to quantify stable sub-surface oil-droplet suspensions, this analysis suggests that the ABS response may be limited within deep water structures where low frequency (long wavelength) acoustic signals are required. Conversely, 38 kHz echo sounders have been proven useful to track sub-surface oil releases (Adams and Socolofsky, 2005).

The goal of this study was to determine the correlation between ABS and oil droplet concentrations under controlled laboratory conditions. The capability to develop quantitative ABS response factors to predict oil droplet concentrations was evaluated. Finally, the measured ABS responses were compared against the theoretical ABS responses inferred from the droplet size distributions to evaluate method sensitivity and potential interferences.

2. Materials and methods

2.1. Experimental design

Echo intensity (EI) responses to standard oil droplet suspensions were measured during three experiments conducted in a laboratory test tank using a 2400-kHz Teledyne RD Instruments StreamPro. For experiment 1, EI responses were collected for six treatments including (a) no-oil control and (b) standard oil droplet suspensions of 6, 12, 18, 24, and 30 μL/L (nominal). For experiments 2 and 3, a sixth standard oil droplet suspension treatment of 36 μL/L was evaluated. The oil droplet suspensions were characterized *in situ* for total droplet volume concentration and droplet size distribution using a LISST-100, Type B (Sequoia Scientific Inc., Bellevue, WA, USA).

The SteamPro was mounted to a rigid support in a down-looking orientation in the tank center with transducer depth set at 5 cm below the water surface. Real time data collection was made with WinRiverII (Teledyne RDI) via a Bluetooth serial connection to a Dell laptop computer with a Windows XP operating system. The StreamPro was configured in WinRiverII to collect echo intensity ensembles (samples) with the following settings; 6 pings/ensemble, ping rate = 2 Hz, depth bin size = 10 cm, number of depth bins = 15, first depth bin = 0.16 m. A separate ensemble file was collected for each standard oil droplet suspension treatment with at least 60 ensembles collected per file. To alleviate variations in incident signal strength resulting from power fluctuations as described by Wall et al. (2006), the StreamPro was connected to a laboratory power supply with operating voltage set to 12.5 VDC.

All echo intensity (*EI*) values from the 4 beams were normalized with respect to beam 1 as previously described (Wall et al., 2006; Fuller, 2011). The normalized *EI* values were converted to acoustic backscatter (ABS) in decibel (dB) units as the product of the *EI* and the Received-Signal-Strength Indicator (RSSI) factor (Wall et al., 2006; Fuller, 2011). The RSSI factor was determined as the slope of the line generated by plotting the normalized *EI* against the sum of the beam spreading and water absorption attenuation values, with respect to depth (Fuller, 2011). The ABS values were then corrected for attenuation due to beam spreading and water absorption (Wall et al., 2006; Deines, 1999; Gartner, 2004; Schulkin and Marsh, 1962). Sediment attenuation evaluated as a function of the droplet size distribution observed at the highest oil concentrations (36 μL/L) was negligible and therefore omitted from ABS data processing (Flammer, 1962; Gartner, 2004).

2.2. Test tank configuration

All tests were conducted in an open-top fiberglass tank (Inside Diameter 3.7 m × Depth 1.7 m). The tank bottom was lined with rubber mats (1.9 cm thick) to minimize acoustic signal reflection and subsequent interference with the StreamPro. The tank was filled with salt water with a salinity = 30 psu verified with a refractometer. The salt water was prepared by filling the tank to capacity with potable water to which 545 kg NaCl (Morton Purex All Purpose, food grade) was added. The tank was then allowed to mix-continuously until salt was completely dissolved. Tank mixing was provided by a 1-Hp pool pump that was plumbed to an octagonal PVC distribution manifold installed on the tank bottom (Fuller, 2011). The manifold contained 32 equally spaced distribution ports (diam-0.7 cm) oriented to direct the water toward the tank center and along the tank bottom. This configuration resulted in an upwelling at the tank center with a down current around the tank circumference. Pump intake was through a 3.7 cm (I.D.) bulkhead fitting located 5 cm above the tank bottom. Pump flow rate was set at 0.17 m^3/s resulting in a tank turnover time of 92 min.

The salt water was recycled between experiments via a 2-stage filtration process. The first filtration stage was provided by a diatomaceous earth filter (Hayward Progrid, Model 3620). Second stage filtration was provided by a sand type filter (Hayward Pro Series, Model S166T) charged with granular activated carbon. To prevent algal growth in tank, the water was treated with an algaecide (Leslie's Swimming Pool Algae Control, LPM Manufacturing, Inc. Phoenix, AZ) at the manufacturer's recommended dosage.

2.3. Mixing shear determination

The oil-droplet size distribution is dependent on the energy dissipation rate (i.e. shear) (Li et al., 2008; Sterling et al., 2004a). Therefore it was necessary to control the mixing power to enable generation of realistic and reproducible oil-droplet size distributions. Following the procedure presented by Sterling et al. (2004a), the experimental test tank mixing was scaled to the mean shear rate, G_m, determined with the Camp and Stein (1943) equation

$$G_m = \left(\frac{Po}{\mu V}\right)^{1/2} \tag{2}$$

where G_m is s^{-1}, Po is watts, μ is 1.002E-3 kg m^{-1} s^{-1}, V (reactor volume) is 16 m^3. Power injected into the test tank by the 1 Hp pump was calculated using Bernoulli's equation

$$\frac{-dW_{a.o}}{dm} = \Delta\left(\frac{P}{\rho} + gz + \frac{U^2}{2}\right) \tag{3}$$

where $W_{a.o}$ is pump work (kg m^2 s^{-2}), m is fluid mass (kg), P is pressure (kg m^{-1} s^{-2}), ρ is water density (kg m^{-3}), g is gravity (m s^{-2}), U is fluid velocity (m s^{-1}), and z is the water surface height (m) (De Nevers, 1991). Given that ΔP and Δz are zero, Eq. (3) may be simplified to

$$\frac{-dW_{a.o}}{dm} = \Delta\left(\frac{U^2}{2}\right) \tag{4}$$

This expression may be converted to units of power by multiplying both sides of the equation by the mass flow rate (kg s^{-1}). Mixing power input to the test tank (Po) was calculated as a function of mass flow rate and water velocity, which were determined using an inline paddle wheel flow meter (Omega Engineering, Inc., Model # FP2020-R) that was installed between the pump and water discharge into the tank. The resultant power values were then substituted into Eq. (2) to determine the respective G_m. All tests were conducted with at G_m = 25 s^{-1}, which was comparable to the shear rates evaluated in oil droplet coalescence studies by Sterling et al. (2004a,b,c, 2005).

2.4. Dispersed oil

All oil droplet suspensions were prepared with artificially-weathered Arabian medium crude oil. The natural weathering of the crude oil was simulated by air stripping the volatile fractions which reduced the volume by 30–35%. The weathered oil had a specific gravity of 0.9129, kinematic viscosity of 102.4 centistokes at 20 °C, and a Reid vapor pressure of 2.1 kPa at 37.8 °C. This oil was premixed with the dispersant Corexit® 9500A (Nalco, Sugar Land, TX) at a 10:1 oil-mass-to-dispersant-mass ratio. Each experimental oil droplet treatment was made by injecting 95 mL of the oil-dispersant mixture (neat) with two 50-mL syringes directly below the water's surface. Each 95 mL oil injection represented a nominal standard oil droplet load equivalent to 6 μL/L. The nominal oil concentration in each treatment was calculated as the sum volume of the oil treatment additions divided by the test tank volume. For Experiment 1, the oil-dispersant mixture was added at the tank center, in the up-welling current. Visual observations combined with the low total volume concentrations indicated that substantial oil volumes remained at the tank surface (i.e. not entrained in the water column). For Experiments 2 and 3, the oil injection location was moved from the tank center to a location adjacent to the tank wall. This location change takes advantage of the down-welling current which provided additional oil residence time in the water column, thereby enhancing overall oil dispersant efficiency as indicated by a higher percentage of the initial oil volume being dispersed. Also, for Experiments 2 and 3, the additional treatment (STD 6, 36 μL/L) was added to evaluate the ABS response over the full linear detection limit of the LISST-100. Each oil-dispersant injection was allowed to mix in the tank for 10 min prior to collecting StreamPro ABS samples and LISST-100 particle size samples. To prevent acoustic interference, the LISST-100 was removed from the tank during ABS sampling with the StreamPro. Thus, sample collection was conducted sequentially, first the StreamPro followed by the LISST-100.

2.5. Volume concentration measurements

Oil droplet volume concentrations and particle size distributions (PSDs) were measured *in situ* with a LISST 100, Type B (Sequoia Scientific, Bellevue, WA, USA.) that measures 32 log-normally-distributed particle size classes with diameters ranging from 1.2 to 250 μm. The LISST was configured to collect 1 sample/ensemble using the LISST MFC Application (Version 1.0.0.1). It was suspended on a chain in a horizontal orientation to reduce settling of suspended particles on optical surfaces. All measurements were taken at 0.65 m below the water surface. All volume concentrations and particles size distributions reported in this study are the mean of 30 ensembles. No attempt was made to quantify the amount of oil adsorbed to the tank surfaces as this study was designed only to evaluate the ABS response to the entrained oil droplet concentration.

3. Results

3.1. Total volume concentrations

The LISST-100 total volume measurements were determined from response to all particles entrained within the water column including oil-droplets, suspended sediments, and bubbles. All measurements were made using a background scatter file collected during the Experiment 1 control (i.e. clean-water no-oil conditions). This was done to directly measure any variations in the experimental droplet distributions between experiments with respect to total volume concentrations and size distribution. Total oil volume concentration was linear with nominal oil loads as indicated by $R^2 > 0.99$ for all three experiments (Fig. 1). Changing the oil injection location from the tank center in Experiment 1 to near the tank wall in Experiments 2 and 3 resulted in more efficient oil dispersion as indicated by the respective increase in the linear regression slopes (Fig. 1). Experiment 2 (square data points) showed an elevated ambient particle concentration of 5 μL/L at nominal oil load = 0 μL/L, compared to Experiments 1 (diamond data points) and 3 (triangle data points) which both show ambient particle concentrations less than 1 μL/L (Fig. 1). The source of the elevated ambient particle load observed in Experiment 2 was not characterized. However, the test tank was located outdoors and subject to contamination from wind-blown particles.

3.2. Particle size distribution (PSD)

The particle size distributions (PSDs) from each experimental experiment were plotted Fig. 2. All particle size distributions were

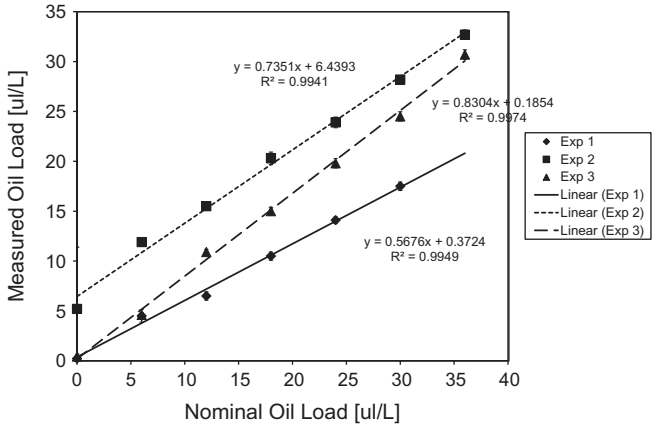

Fig. 1. Nominal vs. measured oil load, as measured by the LISST-100. Error bars represent standard deviation of mean ($n = 30$).

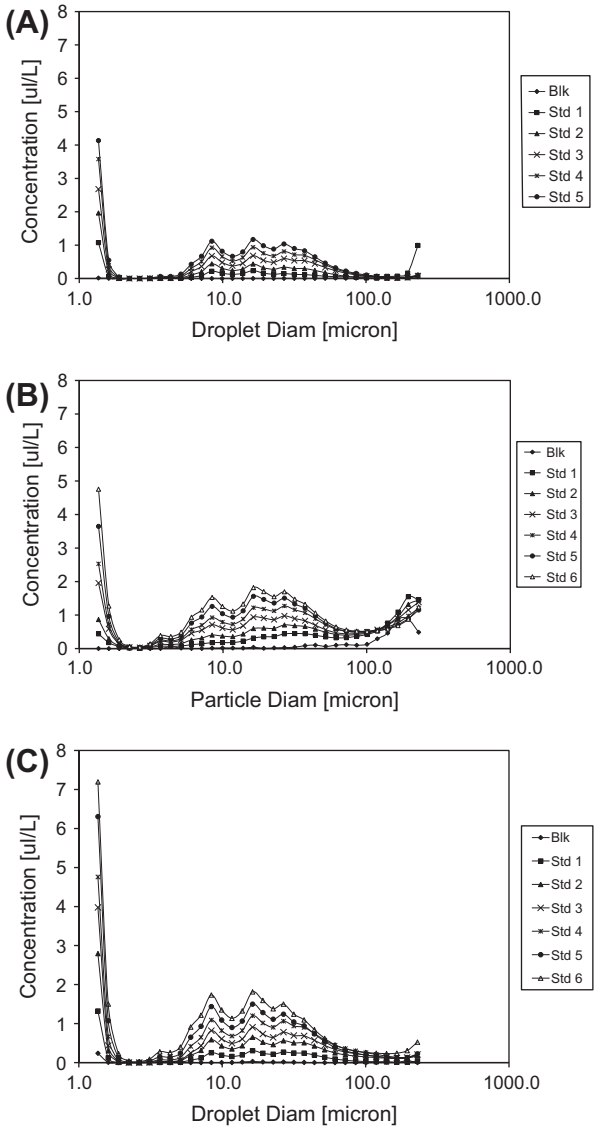

Fig. 2. Oil droplet size distributions measured with LISST-100; (A) Experiment 1, (B) Experiment 2, and (C) Experiment 3.

collected using the background scatter file collected in the test tank for Experiment 1 so that any PSD changes in the no-oil controls could be characterized. Note that the droplet size distribution for Experiment 2 (Fig. 2B) showed an elevated ambient particle load (i.e. no-oil control) with particle diameters greater than 150 μm being retained in all Experiment 2 dispersed oil treatments. Inspection of Experiments 1 and 3 PSDs (Fig. 2A and C) showed elevated large droplet concentrations only with the Experiment 1, Std 1 (6 μL/L, nominal). Neglecting the presence of ambient particle loads, the oil-droplet PSDs were similar to the oil-droplet PSDs generated at $G_m = 20\ s^{-1}$ as presented by Sterling et al. (2004a) with most of the droplets being distributed between 10 and 100 μm. However, one obvious difference is the presence for the large peak occurring at 1.3 μm (Fig. 2A–C), which is not present in the PSDs presented by Sterling et al. (2004a). This difference may be due the scale effects resulting from differences in reactor volume, configuration, and/or mixing method. For clarification, Sterling et al. (2004a) used a rectangular, 32-l reactor, agitated by rotating an impeller with four cylindrical rods evenly staggered throughout the water column. While the mean shear determined for both reactors were similar, localized volumes with high shear in the current reactor configuration, including centrifugal pump, plumbing fixtures, and distribution manifold, may have contributed to the presence of the small oil droplets.

The mean droplet diameter is calculated from the particle size distribution as

$$d_{mean} = \frac{\sum C_i d_i}{C_{total}} \tag{5}$$

where C_i is the particle (droplet) concentration with a diameter d_i and C_{total} is the total volume concentration. To alleviate ambient particle contributions to the mean droplet diameter, the no-oil control PSD from each experiment was subtracted from the respective PSD obtained for each standard oil treatment. Maximum oil droplet diameters in all experiments were less than 100 μm. Therefore, diameters greater than 100 μm were omitted from mean droplet diameter calculations. This omission was justified by evaluating the ratio

$$\frac{VC_{<100\mu m}}{VC_{oil}} \tag{6}$$

where $VC_{<100\mu m}$ is the volume concentration inferred from the PSD < 100 μm, and

$$VC_{oil} = VC_i - VC_{no\text{-}oil} \tag{7}$$

i is the standard oil addition, and *no-oil* represents the no-oil control. The mean ratio (Eq. (6) for all oil standard additions of all 3 experiments was 0.98 ($\sigma = 0.072$), indicating that 98% of the oil-droplets had diameters less than 100 μm. A mean droplet diameter of 18 (±1) μm determined from all experiments and treatments indicates that oil droplet diameters were conserved throughout this study (Fig. 3). Further, the measured oil droplet diameter is comparable to the mean droplet diameter of 17(±6) μm reported by Sterling et al. (2004a) indicating the test tank mixing was scaled appropriately with mean shear (G_m). From the perspective of an ABS evaluation, the reproducible droplet suspensions suggest that the observed ABS responses in each experiment should be similar.

3.3. ABS depth profiles

ABS depth profiles were generated by first correcting the measured ABS for beam spreading and water absorption attenuation as previously described. ABS profiles for no-oil control treatments were omitted as clean water conditions lacked sufficient concentration of scattering particles resulting in a high percentage (on the order of 90%) bad ADCP ensembles. The lowest oil concentration treatments (6 μL/L, nominal) in each experiment resulted in nearly 100% good echo intensity ensembles in all valid depth bins.

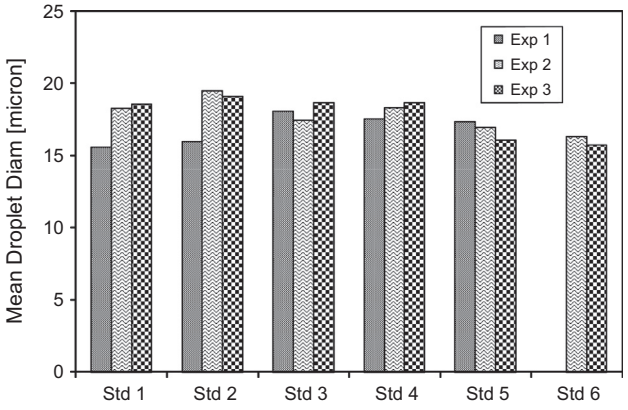

Fig. 3. Mean droplet diameter calculated from PSD less than 100 μm and with ambient particle load subtracted.

A valid depth bin was defined in this study as the first eleven depth bins, representing depths from 0.16 to 1.16 meters, not showing elevated echo intensities resulting from incident signal reflection off tank surfaces. A positive relation is indicated between oil-droplet concentration and the observed ABS (Fig. 4). However, in Experiments 2 and 3 (Fig. 4B and C, respectively) maximum oil loads (36 μL/L, nominal) resulted in no appreciable change in the ABS response relative to the previous oil load (30 μL/L, nominal). Error associated with the ABS corrections for beam spreading and water absorption is apparent in the ABS depth profiles generated for each standard oil addition in all experiments (Fig. 4). Assuming that the oil droplet suspensions were homogenously distributed throughout the tank volume, the corrected ABS depth profiles would exist as a vertical line under ideal conditions. All profiles deviate from vertical with a corrected ABS decline (~0.5–1 dB) between the 0.16 and 0.36 m depth bins and a gradual corrected ABS increase (~0.5–1 dB) between the 0.36 and 1.16 m depth bins (Fig. 4) Despite this error, some inferences may be made from the ABS profiles. The highest ABS (~62 dB) occurred at the highest oil concentration of 17 μL/L measured for Experiment 1, STD 5 (Fig. 4A). However, this oil load is approximately one-half the maximum oil concentration measured in Experiments 2 and 3 that resulted in maximum ABS responses on the order of ~58–59 dB (Figs. 4B–C). This observation suggests the inherent variability of the ABS intensity measurement despite efforts to maintain reproducible conditions by ensuring stable and consistent power to the ADCP and transducer mounting configuration between experiments.

3.4. ABS response curves

No-oil control responses were omitted from all ABS response curves (Fig. 5) due to the lack of sufficient scattering particles required for valid echo intensity measurements. For all experiments, log-linear relationships between ABS and volume concentration were observed as indicated by the Pearson coefficients ($\alpha = 0.05$) of 0.940, 0.938, and 0.881 for Experiments 1, 2, and 3, respectively. Despite the log-linearity, response slopes varied appreciably, between 0.11 and 0.27, suggesting the difficulty associated with obtaining valid calibration coefficients for dispersed oil concentration determinations. Response curves for other valid depth bins (data not shown) were similar to respective experiment depth bin 6 responses.

The oil-droplet characterization indicated that the droplet size distributions were, for the most part, conserved between experiments, with the exception of the ambient concentration of relatively large particles in Experiment 2 (Fig. 2). Assuming that ABS

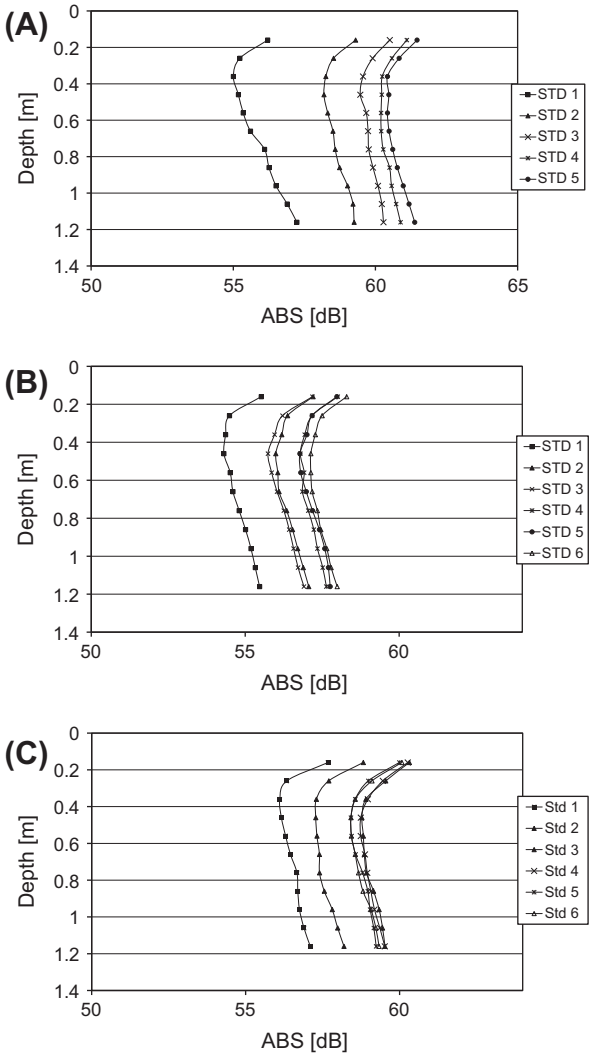

Fig. 4. Corrected ABS depth profiles for each standard addition. Profiles for no-oil controls omitted; (A) Experiment 1, (B) Experiment 2, and (C) Experiment 3.

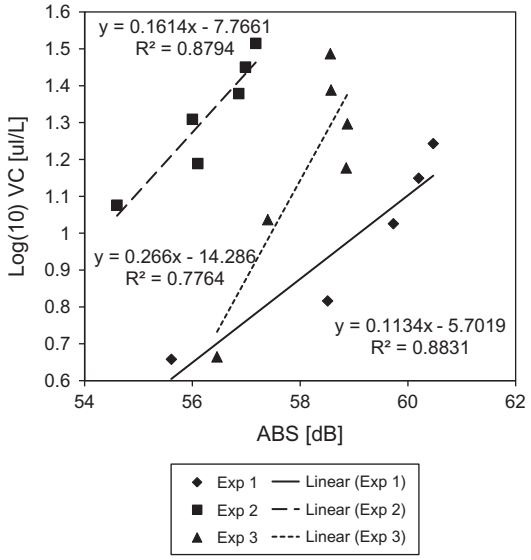

Fig. 5. Depth bin 6 ABS responses to dispersed oil Log(10) volume concentration.

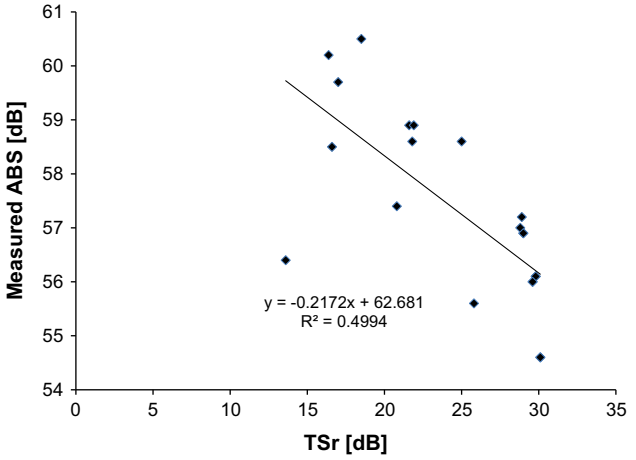

Fig. 6. Rayleigh target strength (TS_R) vs. measured ABS (depth bin 6) for all experiments and conditions. No-oil control responses omitted.

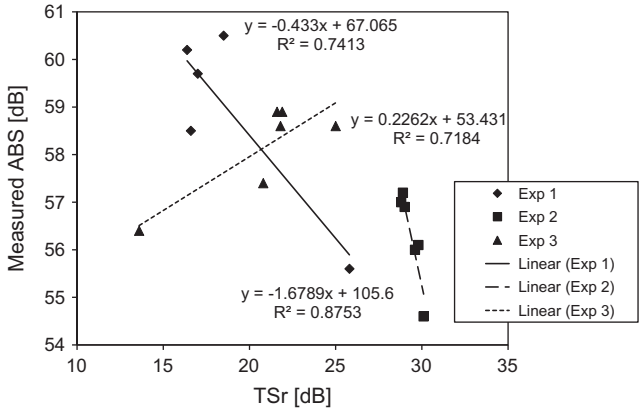

Fig. 7. Measured ABS (depth bin 6) vs. calculated Rayleigh target strength for each experiment. No-oil control responses omitted.

response follows the Raleigh scattering equation (Eq. (1)), this suggests that the measured responses would be proportional to theoretical values determined with the particle size distribution. However, when the measured ABS responses from all experiments are combined (no-oil control values omitted) and plotted against the respective Raleigh target strength (TS_R) the relationship is shown to be inversely proportional as indicated by the negative slope (Fig. 6). Furthermore, no correlation was indicated between the Rayleigh target strength and measured ABS response as indicated with student's T-test with $p = 2.32 \times 10^{-22}$ ($\alpha = 0.05$). This suggests that the observed response variability is not a function of the PSD.

ABS measured by the ADCP is known to vary proportionally to transmit power and transmit length, and is one potential cause of the observed ABS variability. When possible, ABS values should be corrected for these known variances as previously described (Wall et al., 2006). With the StreamPro ADCP, such corrections are not possible as these parameters are not provided in the data output. The primary measure exercised to reduce such variability in the study was the use of a laboratory power supply to alleviate the possibility of variable power associated with standard battery pack operation. However, no measures were available to ensure reproducible transmit length. Further, the ADCP determines water velocities as a function of the Doppler shift which is independent of echo intensity (Personal Communication, Dan Murphy, Teledyne RD Instruments, October 17, 2010). As such, ADCPs are not specifically intended to measure echo intensity.

While the theoretical TS_R does not help explain experiment variability, it can be useful to determine potential interferences. Plotting the ABS responses from each experiment separately against the respective TS_R values (Fig. 7) allows potential interferences to be evaluated. Only Experiment 3 showed an expected positive relationship between TS_R and measured ABS (Fig. 7). Inspection of Experiment 1 (Fig. 7, diamond data points) shows an elevated TS_R at the lowest measured ABS. This data point corresponds to Experiment 1, standard 1 which was characterized with an elevated concentration of droplets at the largest size category = 230 μm (Fig. 2A). This observation indicated the presence of a transient (i.e. not present in latter treatments) scatterer population contributing to the unexpectedly high TS_R value. Similarly, Experiment 2 PSD (Fig. 2B) showed elevated concentrations at the upper end of the size distribution in all experimental conditions (i.e. no-oil control and all dispersed oil standards). Fig. 7 also shows a negative relationship between Experiment 2 (square data points) TS_R and the measured ABS. It is important to notice the small absolute difference in maximum and minimum TS_R values determined for

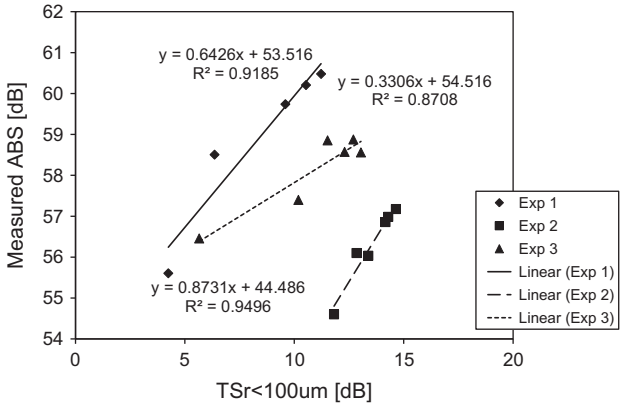

Fig. 8. Measured ABS response (depth bin 6) vs. TS_{Roil} calculated with PSD < 100 μm.

Experiment 2. Considering that TS_R is proportional to the 6th power of the droplet radius as defined by Eq. (1), this indicates that the modeled TS_R is being strongly affected by the relatively high ambient particle load with diameters predominantly greater than 100 μm.

To evaluate the effect of the ambient particles on the TS_R required that the TS_{Roil} be calculated from the PSD less than < 100 μm, where TS_{Roil} is the Raleigh target strength resulting from the oil droplet suspension. Neglecting the PSD > 100 μm in the TS_{Roil} calculations was justified by the previous evaluation of Eq. (6). Plotting TS_{Roil} against the respective measured ABS responses shows positive linear correlations with $R^2 > 0.87$ for all three experiments (Fig. 8). Considering the ambient particle load to be constant within each experiment, this analysis demonstrates that the observed ABS intensity is changing with respect to variable oil-droplet concentrations. This further implies that this methodology has sufficient sensitivity to detect oil-droplet concentration variations even in the presence of relatively large ambient particles with characteristically elevated TS_R compared to the smaller oil-droplets.

4. Conclusions

The observed log-linear ABS responses to oil-droplet volume concentration in each experiment suggest that ABS is a potentially viable remote sensing tool to quantitatively and spatially characterize sub-surface dispersed oil plumes. The inability to generate reproducible slopes demonstrates method variability and indicates

the difficulty associated with producing meaningful response factors required to make field measurements with any precision. However, the strong linear correlations between the observed ABS response and the TS_{Roil} demonstrate that this methodology has the sensitivity required to detect relative changes in the oil-droplet concentrations in the presence of potentially interfering ambient particles. These findings illustrate ABS intensity as a potentially viable technology for quantitative remote detection of sub-surface oil-droplet suspensions. However, further development and field evaluations are required to improve response reproducibility and validate ABS methods as a tool to quantify dispersed oil suspensions. Recognizing these needs, we have conducted field evaluations in the Hudson River, NY where these ABS methods were used to provide suspended sediment concentration values comparable to direct measurement values (Islam et al., Unpublished data). Considering current environmental regulations that prohibit oil discharge into U.S. water ways, field evaluation of these methods to estimate dispersed-oil concentrations is pending the occurrence of a spill-of-opportunity or dispersant field trials in foreign waters. Until this goal is achieved, these findings indicate that ABS can be an effective screening tool to remotely locate potential areas with high oil concentrations for more thorough analysis using alternative methods (i.e. fluorescence coupled with an AUV and/or discrete sampling).

Acknowledgements

We thank the Beacon Institute for Rivers and Estuaries for funding this research.

References

Adams, E.E., Socolofsky, S.A., 2005. Review of: deep oil spill modeling activity supported by the DeepSpill JIP and offshore operators committee, accessed 5 January 2010. <http://www.boemre.gov/tarprojects/377/Adams%20Review%204.pdf>.

Camilli, R., Reddy, C.M., Yoerger, D.R., Van Mooy, B.A.S., Jakuba, M.V., Kinsey, J.C., McIntyre, C.P., Sylva, S.P., Maloney, J.V., 2010. Tracking hydrocarbon plume transport and biodegradation at Deepwater Horizon. ScienceExpress. doi:10.126/science.1195223.

Camp, T.R., Stein, P.C., 1943. Velocity gradients in laboratory and full-scale systems. J. Boston Soc. Civil Eng. ASCE 30, 219–237.

De Nevers, N., 1991. Fluid Mechanics for Chemical Engineers. McGraw-Hill, Boston, MA.

Deines, K.L., 1999. Backscatter estimation using broadband acoustic Doppler current profilers. Available: <http://www.commtec.com/Library/Technical_Papers/RDI/echopaper.pdf>.

Flammer, G.H., 1962. Ultrasonic measurement of suspended sediment. US geological survey, Bulletin 1141-1, US Government Printing Office, Washington, DC.

Fuller, C., 2011. Ecological effects and in-situ detection of particulate contaminants in aqueous environments. Ph.D. Dissertation, Department of Civil Engineering, Texas A&M University, College Station, TX.

Gartner, J.W., 2004. Estimating suspended solids concentrations from backscatter intensity measured by acoustic Doppler current profiler in San Francisco Bay, California. Mar. Geol. 211, 169–187.

Gray, J.R., Gartner, J.W., 2009. Technological advances in suspended-sediment surrogate monitoring, Water Resour. Res. 45, W00D29. doi:10.1029/2008WR007063.

Hamilton, L.J., Shi, Z., Zhang, S.Y., 1998. Acoustic backscatter measurements of estuarine suspended cohesive sediment concentration profiles. J. Coastal Res. 14 (4), 1213–1224.

Hazen, T., Dubinsky, E., DeSantix, T., Andersen, G., Piceno, Y., Singh, N., Jansson, J., Probst, A., Borglin, S., Fortney, J., Stringfellow, W., Bill, M., Conrad, M., Tom, L., Chavarria, K., Alusi, T., Lamendella, R., Joyner, D., Spier, C., Baelum, J., Auer, M., Zemla, M., Charkraborty, R., Sonnenthal, E., D'haeseleer, T., Holman, H., Osman, S., Lu, A., Van Nostrand, J., Deng, Y., Zhou, J., Mason, O., 2010. Deep-sea oil plume enriches indigenous oil-degrading bacteria. Sciencexpress. http://dx.doi.org/10.1126/science.1195979.

Islam, M.S., Bonner, J.S., Page, C.A., 2010. A fixed robotic profiler system to sense real-time episodic pulses in Corpus Christi Bay. Environ. Eng. Sci. 27 (5), 431–440. http://dx.doi.org/10:1089/ees.2010.0006.

Islam, M.S., Bonner, J.S., Fuller, C., Kirkey, W., Unpublished data. Development of surrogate technology using acoustic backscatter for field measurement of suspended solids concentration.

Li, Z., Lee, K., King, T., Boufadel, M., Venosa, A.D., 2008. Assessment of chemical dispersant effectiveness in a wave tank under regular non-breaking and breaking wave conditions. Mar. Pollut. Bull. 56, 903–912.

Lubchenco, J., 2010. Transcript- NOAA administrator's keynote address on NOAA science and the Gulf Oil Spill. Accessed 18 November 2010. <http://www.restorethegulf.gov/release/2010/10/01/transcript-noaa-administrator%E2%80%99s-keynote-address-noaa-science-and-gulf-oil-spill>.

Ojo, T.O., Bonner, J.S., Page, C., 2006. Observations of shear-augmented diffusion processes and evaluation of effective diffusivity from current measurements in Corpus Christi Bay. Continental Shelf Res. 26, 788–803.

Page, C.A., Bonner, J.S., Sumner, P.L., Autenrieth, R.L., 2000. Solubility of petroleum hydrocarbons in oil/water systems. Mar. Chem. 70, 79–87.

RD Instruments, 1996. Acoustic Doppler Current Profiler Principles of Operation, A Practical Primer. RD Instruments, San Diego, CA.

RD Instruments, 2006. StreamPro ADCP Operation Manual. P/N 95B–6003-00. RD Instruments, Poway, CA.

Reichel, G., Nachtnebel, H.P., 1994. Suspended sediment monitoring in a fluvial environment: advantages and limitations applying an acoustic Doppler current profiler. Water Res. 28 (4), 751–761.

Schulkin, M., Marsh, H.W., 1962. Sound absorption in sea water. J. Acoustical Soc. Am. 32 (6), 864.

Smith, S., Greenaway, S., Apeti, D., Mayer, L., Weber, T.C., De Robertis, A., Wright, D., Blankenship, M., Cousins, J., 2010. NOAA ship Thomas Jefferson Deepwater Horizon response mission report, Interim project report-Leg 3, June 15–July 1, 2010. Accessed 18 November 2010. <http://www.noaa.gov/sciencemissions/PDFs/TJ%20Deepwater%20Horizon%20Response%20Project%20Report%20Leg%203_ final.pdf>.

Sterling, M.C., Bonner, J.S., Ernest, A.N.S., Page, C.A., Autenrieth, R. L., 2004a. Chemical dispersant effectiveness testing: influence of droplet coalescence. Mar. Pollut. Bull. 48, 969–977.

Sterling, M.C., Bonner, J.S., Page, C.A., Fuller, C.B., Ernest, A.N., Autenrieth, R.L., 2004b. Modeling crude oil droplet-sediment aggregation in nearshore waters. Environ. Sci. Technol. 38, 4627–4634.

Sterling, M.C., Bonner, J.S., Ernest, A.N.S., Page, C.A., Autenrieth, R. L.,2004c. Characterizing aquatic sediment-oil aggregates using in-situ instruments. Mar. Pollut. Bull. 48, 533–542.

Sterling, M.C., Bonner, J.S., Ernest, A.N.S., Page, C.A., Autenrieth, R. L., 2005. Application of fractal flocculation and vertical transport model to aquatic sol-sediment systems. Water Res. 39, 1818–1830.

Teledyne RD Instruments, 2010. Teledyne RDI's Tech Tips. Accessed 18 October 2010. <http://www.rdinstruments.com/tips/tips_archive/pharray_0203.aspx>.

Urick, R.J., 1983. Principles of Underwater Sound. McGraw-Hill Book Company, New York, NY.

Wall, G.R., Nystom, E.A., Litten, S., 2006. Use of an ADCP to compute suspended sediment discharge in the tidal Hudson River, New York: US geological survey scientific investigations report 2006-5055. Accessed 22 February 2011. <http://pubs.usgs.gov/sir/2006/5055/pdf/SIR2006-5055.pdf>.